The Journal of Experimental Biology 212, 1191-1201
Published by The Company of Biologists 2009
doi:10.1242/jeb.024166

Quantitative analysis of sex-pheromone coding in the antennal lobe of the moth *Agrotis ipsilon*: a tool to study network plasticity

David Jarriault, Christophe Gadenne, Jean-Pierre Rospars and Sylvia Anton*
INRA, UMR1272, Physiologie de l'Insecte: Signalisation et Communication, Versailles, F-78000, France
*Author for correspondence (e-mail: santon@versailles.inra.fr)

Accepted 20 January 2009

SUMMARY

To find a mating partner, moths rely on pheromone communication. Released in very low amounts, female sex pheromones are used by males to identify and localize females. Depending on the physiological state (i.e. age, reproductive state), the olfactory system of the males of the noctuid moth *Agrotis ipsilon* is 'switched on or off'. To understand the neural basis of this behavioural plasticity, we performed a detailed characterization of the qualitative, quantitative and temporal aspects of pheromone coding in the primary centre of integration of pheromonal information, the macroglomerular complex (MGC) of the antennal lobe. MGC neurons were intracellularly recorded and stained in sexually mature virgin males. When stimulating antennae of males with the three main components of the female pheromone blend, most of the neurons showed a biphasic excitatory–inhibitory response. Although they showed different preferences, 80% of the neurons responded at least to the main pheromone component (*Z*-7-dodecenyl acetate). Six stained neurons responding to this component had their dendrites in the largest MGC glomerulus. Changes in the stimulus intensity and duration affected the excitatory phase but not the inhibitory phase properties. The stimulus intensity was shown to be encoded in the firing frequency, the number of spikes and the latency of the excitatory phase, whereas the stimulus duration only changed its duration. We conclude that the inhibitory input provided by local interneurons following the excitatory phase might not contribute directly to the encoding of stimulus characteristics. The data presented will serve as a basis for comparison with those of immature and mated males.

Key words: olfactory coding, moth, antennal lobe, sex-pheromone, projection neuron, spike train analysis.

INTRODUCTION

Olfaction is an ancestral sense, which plays a major role in the adaptation of both vertebrates and invertebrates to their environment. Odour recognition is essential to vital behaviours like feeding, reproduction and social communication. The sex pheromone communication of moths offers a favourable system for the study of the neural basis of this sensory modality because of its relative simplicity, specificity and sensitivity, with specialized and easily accessible neurons responding to only a few pheromone components (Kay and Stopfer, 2006; Mustaparta, 1996).

The pheromone signal emitted by female moths is a blend characterized by the nature of its components, their amount, their specific ratio and their spatiotemporal pattern. By detecting and processing these qualitative and quantitative aspects of the species-specific pheromone signal, a male moth is able to identify and localize a conspecific female (Johansson and Jones, 2007).

The pheromones are detected by male antennal receptor neurons and the information is transferred and integrated first in the antennal lobes (AL). The AL, which are part of the deutocerebrum, are organized in glomeruli, spherical neuropils separated by glial cells (Anton and Homberg, 1999). The glomeruli contain the synaptic connections between peripheral and central neurons. The input signal from the peripheral olfactory receptor neurons (ORN) is integrated in the AL by interactions with local neurons (LN) and projection neurons (PN) and modulated by centrifugal neurons. PN transfer the integrated information to higher processing centres in the protocerebrum (for a review, see Anton and Homberg, 1999).

Moths, such as noctuid species, which rely on sex-pheromone communication, show a sexual dimorphism in their AL structure. Male AL have enlarged glomeruli that collectively form the macroglomerular complex (MGC) (for a review, see Rospars, 1988). The MGC glomeruli receive exclusive input from sex-pheromone receptor neurons (e.g. Hansson et al., 1995).

AL neuron responses depend not only on their intrinsic properties but also on synaptic interactions with the central network. The ORN population from which PN receive their input, directly or indirectly, determines their specificity. Both labelled line and across-fibre processing have been found in the pheromone system of several moth species such as *Manduca sexta*, *Spodoptera littoralis*, *Heliothis* sp. and *Agrotis segetum* (reviewed by Hansson and Christensen, 1999; Mustaparta, 1996). Contrary to the high degree of specificity of ORN responding to pheromones, MGC neurons can respond to more than one pheromone component. Moreover, the response specificity of MGC neurons decreases with increasing concentrations (Anton et al., 1997; Hartlieb et al., 1997). ORN, as well as PN, respond to increasing pheromone concentrations in a dose-dependent manner (Boeckh and Selsam, 1984; Christensen et al., 1991; Hartlieb et al., 1997; Kanzaki et al., 1989). Therefore, qualitative and quantitative aspects of the pheromonal signal are not processed independently in the MGC. Moreover, temporal aspects of the signal are also differentially encoded depending on the components and the dose at which they are detected. In *M. sexta*, the sensitivity of PN and their ability to encode the temporal structure of the stimulus were higher for the pheromone blend than for single components (Heinbockel et al., 2004). In the noctuid moth *A. segetum*, however,

no difference in the capacity to follow pulsed stimuli at frequencies up to 10 Hz was found between responses to single components and the blend (Lei and Hansson, 1999).

In addition to the pheromone signal properties, the physiological state of the animal also has to be taken into account in the study of central sex-pheromone processing. Indeed, depending on their age or reproductive state, *Agrotis ipsilon* male moths show different behavioural responses to the three-component pheromone blend emitted by the females. Age differences are also present in the sensitivity of their MGC neurons (Anton and Gadenne, 1999; Gadenne et al., 2001; Gadenne et al., 1993).

In the framework of our ongoing study of the neural mechanisms underlying sensitivity changes of the olfactory network during maturation and in relation to the reproductive state, we first quantitatively studied the olfactory coding of the three main features of the pheromonal signal (i.e. the nature of the components, the intensity and the temporal pattern) in single MGC neurons of virgin sexually mature males, using intracellular recording and staining techniques.

MATERIALS AND METHODS

Insect preparation

Larvae of *Agrotis ipsilon* Hufnagel (Lepidoptera: Noctuidae) were reared on an artificial diet (Poitout and Buès, 1974) and maintained in individual plastic cups until pupation at 23±1°C and 50±5% relative humidity under a long-day reversed photoperiod (16 h:8 h L:D photoperiod). Pupae were sexed, and adult males were dated and kept separately from females in plastic boxes and had free access to a 20% sucrose solution. Experiments were performed during the scotophase on non-anesthetized animals. Virgin 5-day-old (sexually mature) males were mounted in a plastic pipette tip with the head protruding. The cuticle, tracheal sacs and muscles were removed from the front of the head to expose the brain. One AL was desheathed to facilitate microelectrode penetration. The preparation was then superfused with a saline solution containing 150 mmol l^{-1} NaCl, 3 mmol l^{-1} $CaCl_2$, 3 mmol l^{-1} KCl, 10 mmol l^{-1} *N*-Tris-methyl-2-aminoethanesulfonic acid buffer and 25 mmol l^{-1} sucrose (pH 6.9) (Christensen and Hildebrand, 1987).

Stimulation

The pheromone blend of *A. ipsilon* consists of three main components: *cis*-7-dodecenyl acetate (Z7-12:OAc), *cis*-9-tetradecenyl acetate (Z9-14:OAc) and *cis*-11-hexadecenyl acetate (Z11-16:OAc) (Gemeno and Haynes, 1998; Picimbon et al., 1997). A blend of these three pheromone components in the ratio 4:1:4 was the most attractive for males in a wind tunnel (Causse et al., 1988; Wakamura et al., 1986). We used the single components and their blend, diluted in hexane at doses ranging from 1 pg to 10 ng on filter paper. For the blend, the doses mentioned refer to the amount of Z7-12:OAc; for example, a 1 ng-blend stimulus was prepared with 1 ng Z7-12:OAc, 0.25 ng Z9-14:OAc and 1 ng Z11-16:OAc. As blank stimulus, we used hexane. All stimuli were presented after a minimum evaporation time of 30 min. A constant charcoal-filtered and humidified airflow was blown over the antenna through a glass tube (inner diameter 8 mm) whose outlet surrounded the tip of the antenna. The continuous airflow velocity was 0.3 m s^{-1} (17 ml s^{-1}). Stimuli were presented by inserting a Pasteur pipette, containing the odour-impregnated filter paper, in the glass tube 20 cm from the antenna. An air pulse (7 ml s^{-1}) was blown through the Pasteur pipette, loaded with single pheromone components, the blend or hexane only by means of a stimulation device (CS 55, Syntech, Kirchzarten, Germany). The stimulus was delivered for 200 ms when testing the dose–response relation, and for at least three durations from the following list when testing the relationship between the stimulus duration and the response duration: 100, 200, 300, 400, 500, 600, 700, 800, 1000, 1200, 1300, 1500, 2000 ms. In order to keep the mechanical component of the stimulation to a minimum, an airflow of the same velocity as the stimulus was permanently added to the continuous airflow and removed during the stimulation. The odours were presented randomly, separated by interstimulus intervals of at least 10 s, with lower stimulus loads tested first.

Intracellular recording and data analysis

Intracellular recordings were performed according to standard methods (Christensen and Hildebrand, 1987). The tip of each glass microelectrode was filled with either 4% Lucifer Yellow CH (in distilled water; Sigma-Aldrich, Saint-Quentin Fallavier, France) or Neurobiotin™ (in 0.25 mol l^{-1} KCl; Abcys, Paris, France), and then the shaft was filled, respectively, with 2 mol l^{-1} LiCl or 3 mol l^{-1} KCl. Electrodes had resistances of 150–200 MΩ, measured in the extracellular medium. The micro-electrode was located near the synaptic neuropil of the MGC, which implies that the recordings were made from primary neurites, axons or dendrites of AL neurons near the MGC and neurons were identified *a posteriori*. After establishing intracellular contact, the activity of the penetrated neuron was monitored before, during and after stimulation of the ipsilateral antenna, using Autospike software (Syntech, Kirchzarten, Germany). Recorded signals were amplified with an Axoclamp-2B amplifier (Axon Instruments, Foster City, CA, USA) and subsequently digitized and analyzed with Autospike. Compiled data files of the recordings were exported as text files, then read in Matlab (The MathWorks, Inc., Natick, MA, USA) for analysis. The duration, latency and frequency of the action potential responses to odorant stimulation were quantified as described below.

Response duration

The end of the excitatory phase was in most cases well defined by an inhibitory phase (in which no spikes were generated). We defined the duration of the excitatory phase as the time difference between the first spike and the last spike of this phase (Fig. 1A). Similarly, we defined the duration of the inhibitory phase as the time difference between the last spike of the excitatory phase and the next spike (Fig. 1A), signalling the return to spontaneous activity (see Results). Unilateral paired *t*-tests were performed to compare responses between two successive doses. Pearson's correlation coefficient was used to test the correlation between excitatory/inhibitory phase duration and stimulus duration or dose and between spike frequency and stimulus duration. The Mann–Whitney test was used to compare spike frequencies evoked by stimuli of 500 ms and 800 ms duration. The phasic and tonic parts of the responses were analysed in two 200-ms bins in the response: the first, 200 ms after the stimulus onset, and the second, 500 ms after the stimulus onset, for both responses to 500-ms and 800-ms stimuli (see Results) (Fig. 11).

Response latency

We quantified the response latency in two ways. First, we determined visually the first spike of the response by taking into account the beginning of the decrease of the interspike intervals (ISIs) with respect to the spontaneous activity and the depolarization with respect to the resting potential (Fig. 1A). We defined the corresponding latency (L_0) as the time elapsed from the onset of the stimulation to this first spike. This latency includes the delay of the stimulus delivery caused by the stimulation apparatus but,

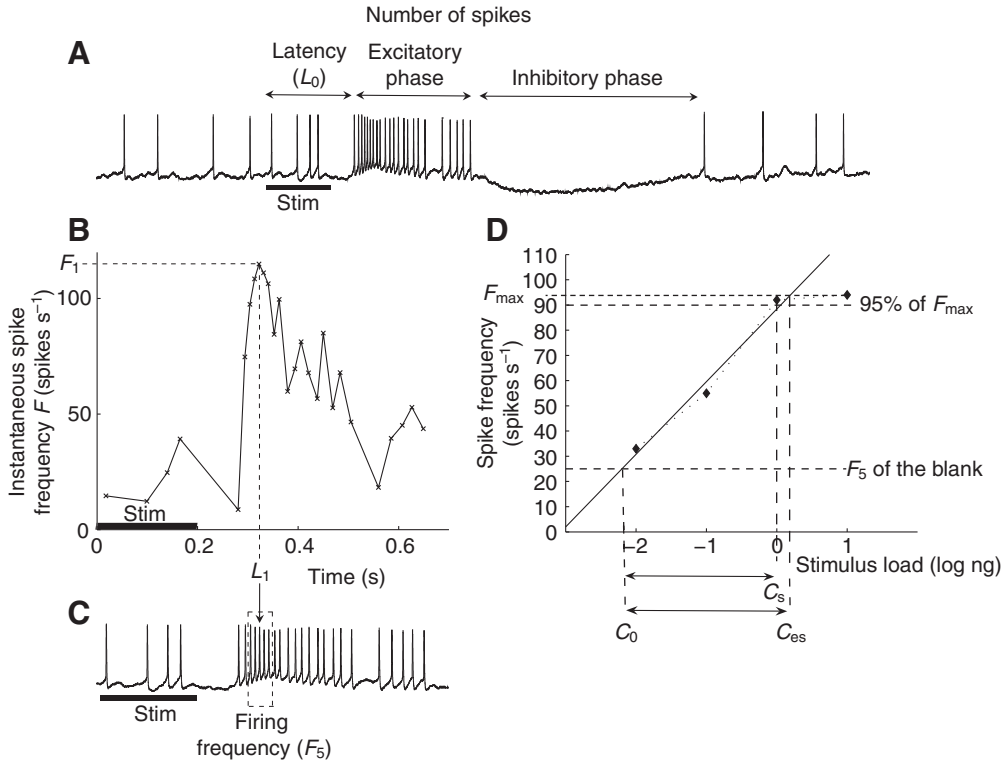

Fig. 1. Definition of the variables used to quantify the responses of macroglomerular complex (MGC) neurons. (A) Example of a recorded spike train during 500 ms before and 2 s after the stimulation. L_0 is the latency of the first spike. (B) Plot of the instantaneous spike frequency F as a function of time after stimulus onset. F was calculated as $1/(t_i–t_{i–1})$, where t_i is the time of occurrence of the spike i. F_1 is the maximum instantaneous spike frequency, and L_1 is the latency of F_1. (C) The firing frequency (F_5) is the mean of the instantaneous spike frequency of five spikes surrounding and including the shortest interspike interval (ISI) ($1/F_1$). (D) Definition of the quantities used to characterize the dose–response plots. A line was fitted to the rising part of the curve. The stimulus load at threshold (C_0) was taken as the dose at which the fitted line reached the blank frequency. The stimulus loads at saturation were taken, respectively, as the first dose eliciting 95% of F_{max} (C_s) or as the dose at which the fitted line reached the maximum firing frequency F_{max} (C_{es}). The horizontal bars (Stim) in A–C indicate the stimulus duration (200 ms).

because the pheromone release is always at the same distance (20 cm from the antenna), any variation is due to delays in transduction, conduction and synaptic transmission. Second, we considered L_1 as the time elapsed from the stimulus onset to the time of occurrence of the spike with maximum instantaneous frequency F_1 (Fig. 1B).

Spike frequency

We quantified the spike frequency in two different ways. First, we determined F_1, the maximum instantaneous spike frequency in the 2 s following the stimulus onset (Fig. 1B). Second, we selected the two ISIs preceding F_1 and the two following ones (Fig. 1C). We calculated the corresponding firing frequency (F_5) as the mean of the inverses of these five ISIs, from which we subtracted the mean spontaneous activity during 1.5 s before the onset of stimulation. F_5 was found to be less variable across neurons than F_1 or any other quantitative expression of response intensity.

Dose–frequency curve

The dependency of response frequency, latency and duration on the dose of the pheromone stimulus was studied. We paid special attention to the sigmoid relationship between dose and spike frequency (Fig. 1D). This sigmoid curve can be characterized by three quantities: the maximum firing frequencies at high pheromone load (F_{max}), the stimulus load at threshold (C_0) and the stimulus load at saturation where the firing rate reaches 95% of F_{max} (C_s). The rising part of the dose–frequency curves can be well approximated by a linear function calculated from the determined spike frequencies up to C_s (this is the dynamic range). Because the range of stimulus loads used did not allow us to determine both threshold and saturation for all neurons, these two parameters were estimated by extrapolating the previously obtained linear regression line. The threshold (C_0) was determined as the stimulus load at which the fitted line reaches a firing frequency equal to that of the blank stimulus. The saturation was determined in two different ways. It was either estimated by the stimulus load (C_{es}) at which the fitted line reaches F_{max} or, on a smaller subset of neurons, as the stimulus load (C_s) eliciting 95% of F_{max}. The dynamic range was then either the difference between C_{es} or C_s and the estimated threshold C_0.

Intracellular staining and laser scanning microscopy

At the end of the recording, neurons were injected iontophoretically with Lucifer Yellow CH by a constant hyperpolarizing current or with Neurobiotin™ by a constant depolarizing current (~0.5 nA in both cases) for 3–10 min. All brains were fixed in 4% buffered formaldehyde for at least 1 h at room temperature. After fixation, the brains were washed with a saline solution (see above for composition) and directly stored in mounting medium (Vectashield H-1000; Vector Laboratories, Burlingame, MA, USA) when stained with Lucifer Yellow CH. When stained with Neurobiotin™, the brains were washed in Millonig's buffer (16 mmol l^{-1} NaH_2PO_4, 10 mmol l^{-1} NaOH, 38 mmol l^{-1} sucrose, pH 7.2) (Millonig's with 0.25% Triton-X) and then dehydrated and rehydrated in an ethanol series and propylene oxide to make membranes more permeable. The brains were incubated in Avidin–Neutravidin–Oregon Green conjugate (Molecular Probes, Cergy-Pontoise, France) diluted at 1:40 in Millonig's buffer overnight at 4°C. The brains were then washed three times in Millonig's buffer and transferred in Vectashield mounting medium. The brains were optically sectioned as whole mounts in a laser-scanning confocal microscope (Leica SP2 AOBS; Leica microsystèmes SAS, Rueil-Malmaison, France) equipped with an argon/neon laser and a 10× dry objective. Each brain was scanned frontally, centred on the AL with a 1.5-μm step size for detailed imaging. Image stacks were analysed by scrolling through optical sections to identify the dendritic arborisation area. A maximum projection of the image stack was performed with Leica Confocal Software Lite (Leica Microsystems, Heidelberg, Manheim, Germany) to analyse the gross anatomy of PN, and three-

Table 1. Quantitative analysis of projection neuron responses to sex pheromone components and blend in the moth *Agrotis ipsilon*: experimental design and sample size

	Specificity	Intensity	Duration
Stimuli			
Components	Z7-12:OAc Z9-14:OAc Z11-16:OAc (+ Blend)	Z7-12:OAc	Z7-12:OAc
Doses	0.01 ng	0.01, 0.1, 1, 10 ng	0.01–1 ng
Durations	200 ms	200 ms	100–2000 ms
Number of animals	69	35	16
Total number of neurons	157	68	26
Complete record sets*	93[a] (68)[†]	29[b]	17[c]

*A record set was complete when a neuron was tested [a] with all three single components, [b] at all four doses or [c] at two or more durations, depending on the coding aspect studied.
[†]Numbers in parentheses are for the blend of all three components.

dimensional reconstructions of individual neurons were done using Amira 3.1 software (Visage Imaging, Berlin, Germany).

RESULTS

Characteristics of MGC-neuron response patterns

The different aspects of sex pheromone coding in *A. ipsilon* were evaluated during three experimental sessions, in which either the nature of the compounds, the stimulus load or the duration of the stimulation were changed. The numbers of neurons recorded in these three sessions are given in Table 1. The recorded neurons were spontaneously spiking at about 20 spikes s^{-1} (mean ± s.d.=22.8±14.6 spikes s^{-1}, 89 out of all recorded neurons). Contact with neurons was usually kept for 5–10 min.

Different patterns of neuronal responses occurred after stimulation with pheromone components. The most common was composed of an excitatory phase followed by an inhibitory phase (97% of all the recorded neurons) (Fig. 2). The excitatory phase showed an increase in firing rate accompanied by a depolarization of the membrane, whereas the inhibitory phase was characterized by an absence of spikes accompanied by a hyperpolarization (Fig. 2). The increase in spike frequency occurred mainly at the beginning of the excitatory phase, after which the spike frequency decreased and kept a value above the spontaneous activity in the remainder of the excitatory phase (see examples in Fig. 8 and Fig. 11). Seventy-two percent of the neurons with a complete record set responded to the blank (hexane and clean air) stimulation, showing the existence of a mechano-sensory input in spite of the airflow compensation used (Fig. 3). The response to the blank presented a pattern similar to that of the pheromone response. In some cases, however, the excitatory phase was shorter than for pheromone responses, and a few spikes occurred during the inhibitory phase (Fig. 3).

In the remaining 3% of the responding neurons, different patterns were observed. In three neurons, the response was a long excitatory phase, after which the frequency slowly decreased down to the level of spontaneous activity (data not shown). In two other neurons, the excitatory phase was preceded by an inhibitory phase (data not shown). Additionally, two neurons responded with an inhibitory phase response only (Fig. 4).

Odour quality coding

In the first experimental session, the three components of the female blend were tested at 0.01 ng during 200 ms on 157 neurons in 69 animals to characterize their specificity. In this sample, 116 neurons responded to at least one of the compounds but only 93 recordings presented sufficient data to analyse the specificity of the recorded neurons. Among these 93 neurons, 47 responded with a high specificity to the main component of the female blend, Z7-12:OAc, 15 neurons to Z9-14:OAc and 1 neuron to Z11-16:OAc (Fig. 5). Similar responses to the three compounds were found in 19 neurons. The remaining neurons responded equally to two of the three compounds (Fig. 5). Responses were obtained in all neurons tested additionally with the blend (68/93). When a neuron responded to more than one component, the previously described response pattern was conserved, but in some cases the spike frequency (F_1 and F_5) or the latency (L_0 and L_1) changed (Fig. 6).

Odour intensity coding

Twenty-nine neurons were tested successfully for their responses to increasing stimulus loads in a range from 0.01 ng to 10 ng of the main pheromone component, Z7-12:Oac, with a constant stimulus duration of 200 ms. These 29 neurons presented an excitatory–inhibitory response for the four tested doses (Fig. 7). The subdivision of the excitatory phase into a phasic and a tonic part was more visible at high stimulus load (Fig. 8; see also Fig. 11). Different variables

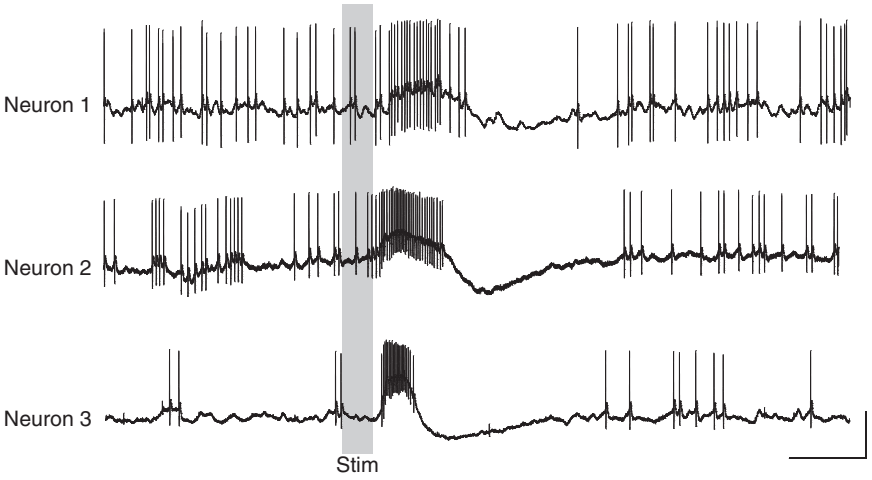

Fig. 2. Typical response pattern of three pheromone-responding macroglomerular complex (MGC) neurons in three different *A. ipsilon* males. Neurons were stimulated with 0.1 ng of the main pheromone component, Z7-12:OAc. Note the different spontaneous activity rates but a common pattern of excitation followed by an inhibitory phase across different neurons. The grey bar indicates the time during which the stimulus was applied (200 ms). Horizontal scale bar, 500 ms; vertical scale bar, 8 mV.

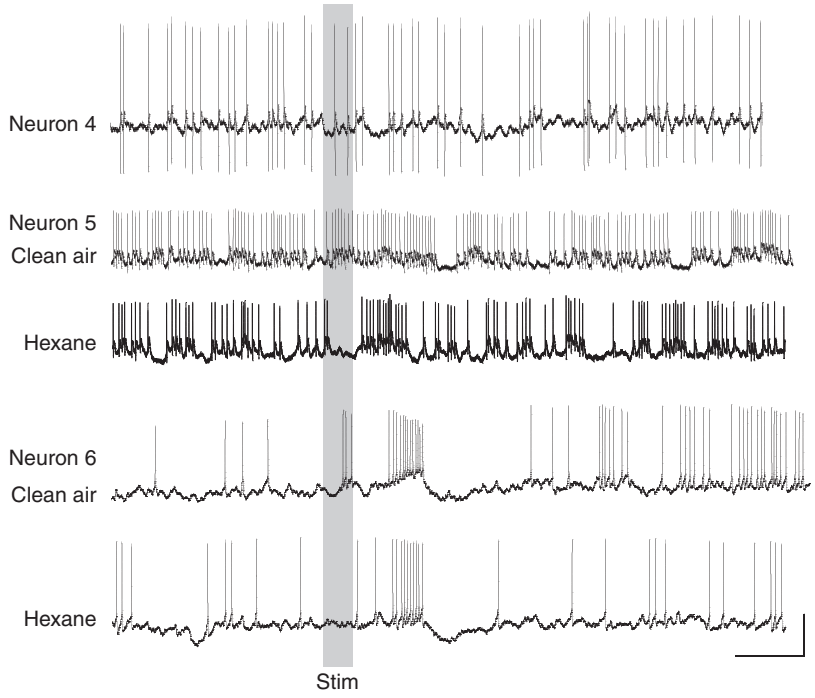

Fig. 3. Responses of three pheromone-responding macroglomerular complex (MGC) neurons to blank stimuli (hexane and clean air) in three different males. Whereas some neurons (neuron 4) did not respond to either hexane or clean air stimulation, others increased their spike frequency slightly (neuron 5) or showed a biphasic response pattern as for the pheromone responses (neuron 6). Similar responses to hexane and clean air indicate the mechanosensory origin of the blank responses. The grey bar indicates the time during which the stimulus was applied (200 ms). Horizontal scale bar, 500 ms; vertical scale bar, 4 mV.

were analyzed to characterize the response pattern as a function of the stimulus load (Figs 1 and 9) and to deduce physiological characteristics of the neurons (Table 2).

The mean stimulus loads at estimated threshold (C_0) and saturation (C_{es}) were calculated for 22 out of the 29 analysed neurons at 0.005 ng and 9.8 ng, respectively (Table 2). The mean stimulus load at observed saturation (C_s) was measured for 17 out of these 29 neurons at 0.6 ng. The dynamic ranges calculated as the differences between either C_s or C_{es} and C_0 were, respectively, 2.6 and ≥3.5 log ng (Table 2). With increasing stimulus loads, the firing frequency (F_5) (Fig. 9A) and the number of spikes (Fig. 9B) increased with the first three doses (t-tests for F_5 and number of spikes, between 0.01 ng and 0.1 ng, t=3.70, P<0.001 and t=3.41, P<0.01, respectively; between 0.1 ng and 1 ng, t=4.13, P<0.001 and t=2.50, P<0.05, respectively) and stabilized (t-test for F_5, between 1 ng and 10 ng, t=0.83, n.s.) or slightly decreased (t-test for the number of spikes, between 1 ng and 10 ng, t=4.68, P<0.001) for the 10 ng dose (Fig. 9A,B). The maximum values attained near saturation for F_5 and the number of spikes in the excitatory phase were, respectively, 114 spikes s^{-1} and 33 spikes (Table 2).

Both the latency of the minimum ISI (L_1) and, to a lesser extent, the latency of the first spike (L_0) decreased with increasing stimulus loads, and no plateau was attained (t-tests for L_1 and L_0, between 0.01 ng and 0.1 ng, t=3.34, P<0.01 and t=2.55, P<0.05, respectively; between 0.1 ng and 1 ng, t=6.31, P<0.001 and t=4.20, P<0.001, respectively; between 1 ng and 10 ng, t=2.52, P<0.05 and t=2.52, P<0.05, respectively) (Fig. 9C,D). For both parameters, the decrease was more pronounced for the first three doses than for the 10 ng dose. In this range of stimulus loads, the minimum latency was 241 ms (Table 2).

The durations of the excitatory and inhibitory phases were, on average, 356±11 ms and 655±30 ms, respectively (Table 2). The duration of these phases was not correlated with the dose (Fig. 9E,F) (Pearson's r=–0.29, n.s. and Pearson's r=0.03, n.s., respectively). The excitatory phase was, on average, 156±11 ms (mean ± s.e.m.) longer than the stimulus duration. The variability of the phase durations among neurons was higher for the inhibitory phase than for the excitatory phase (Fig. 9E,F).

Temporal coding

Seventeen neurons were tested for their response to increasing stimulus durations (from 100 ms to 2 s) in 16 animals (see Materials and methods for details). Experiments were performed with the main pheromone compound (Z7-12:OAc) at three doses: 0.01 ng, 0.1 ng and 1 ng (each neuron was tested at a single stimulus load and with 2–5 durations) and data were pooled because the response duration was found to be independent of the dose. The duration of the excitatory phase increased linearly with the stimulus duration (17 neurons; Pearson's r=0.98, P<0.001) (Fig. 10A). The excitatory phase duration was, on average, 59±10 ms longer than the tested

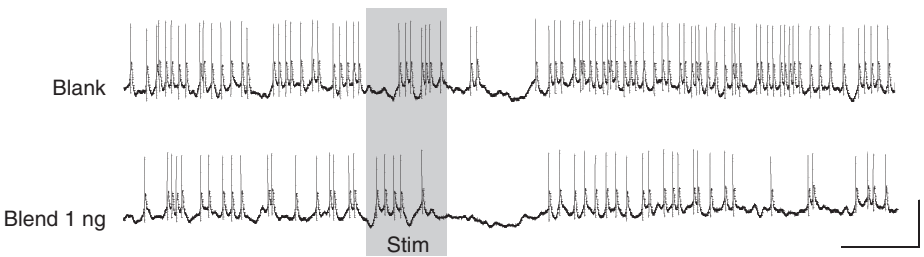

Fig. 4. Responses of a neuron inhibited by the pheromone. The neuron was stimulated with 1 ng of the blend. The grey bar indicates the stimulus duration (500 ms). Horizontal scale bar, 500 ms; vertical scale bar, 4 mV.

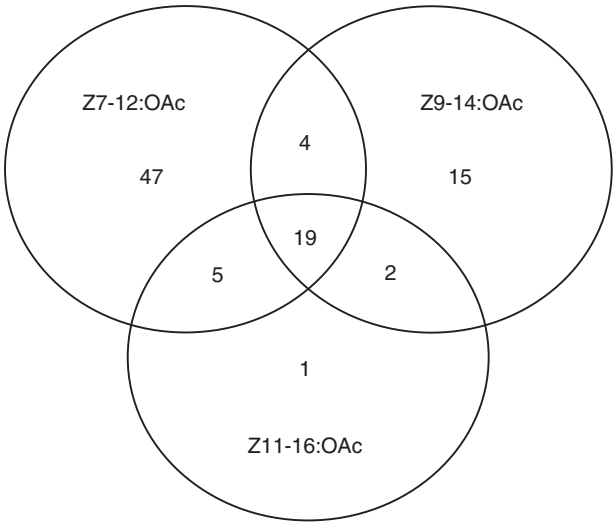

Fig. 5. Response specificity of 93 macroglomerular complex (MGC) neurons for the three components of the pheromone blend. Neurons were stimulated with the three components of the blend separately at the same stimulus load (0.01 ng). Neurons responding specifically to Z7-12:OAc were encountered more often than neurons responding specifically to the two other compounds. Nineteen neurons (20%) responded to all three compounds, and a few neurons responded to different combinations of two of the three compounds.

stimulus. The duration of the inhibitory phase was not correlated with the stimulus duration (15 neurons; Pearson's r=–0.01, n.s.) and varied highly across neurons for a given stimulus duration (Fig. 10B). The division of the excitatory response into a phasic and a tonic part was clearer with long stimuli (>500 ms; Fig. 11). The spike frequencies measured in two 200-ms bins, one in the phasic and the other in the tonic part of the response, were 107±5 spikes s^{-1} and 56±9 spikes s^{-1}, respectively, for a 800-ms stimulus. When comparing the spike frequencies in these two bins between 500-ms and 800-ms stimuli, no statistical differences were found (phasic part, Mann–Whitney U=36, P=0.48; tonic part, Mann–Whitney U=35, P=0.48). Moreover, the firing frequency (F_5), which characterizes the phasic part, did not vary with the stimulus duration (data not shown) (Pearson's r=–0.21, n.s.), showing that changes in stimulus duration do not affect the spike frequency.

Anatomy

Twenty-six out of 106 attempted stainings were successful. All neurons arborised within the MGC glomeruli, previously described by Gemeno et al. (Gemeno et al., 1998) and Greiner et al. (Greiner et al., 2004) (Fig. 12). In 13 stained neurons, MGC arborisations were mainly confined to the largest unit, the cumulus, whereas for the remaining preparations, arborisations could not be unambiguously attributed to a specific glomerulus. In 15 preparations, the axon leaving the AL was visible. Clearly stained axonal arborisations within the protocerebrum were found in two preparations (Fig. 12). Fifteen neurons had their cell body located in the medial cell body cluster of the AL (Fig. 12). In the remaining preparations, the cell body was not visible. Six neurons tuned to the main component (Z7-12:OAc) had arborisations in the cumulus. All stained neurons, except one, responded to the pheromone with the typical response pattern previously described. The remaining neuron presented only an excitatory phase, had its cell body in the medial cell body cluster and its arborisations in the cumulus.

DISCUSSION

We precisely characterized MGC neuron responses of sexually mature, virgin, inexperienced *A. ipsilon* males to sex pheromones as a first step to understand the pheromone-processing AL network.

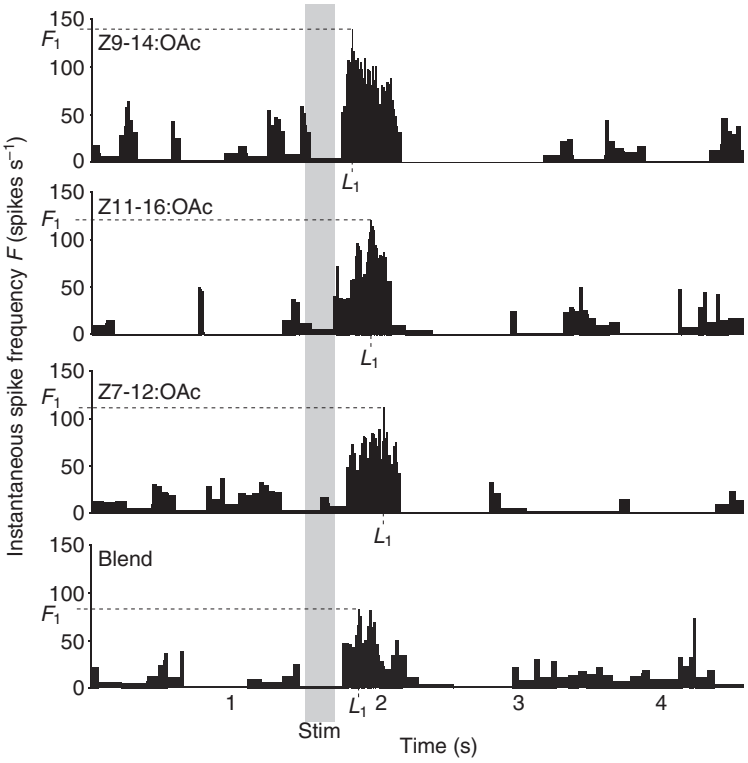

Fig. 6. Histograms of instantaneous spike frequencies, F (as defined in Fig. 1B), of a generalist macroglomerular complex (MGC) neuron responding to the three pheromone components (Z7-12:OAc, Z9-14:OAc, Z11-16:OAc) and their blend (4:1:4). All components were tested at the same stimulus load (0.01 ng). The latency of the maximum instantaneous spike frequency (L_1, dotted lines) is shorter for Z9-14:OAc than for the other components. Spike frequencies are higher for Z9-14:OAc and Z11-16:OAc than for Z7-12:OAc and the blend. The grey bar indicates the time during which the compound was applied (200 ms).

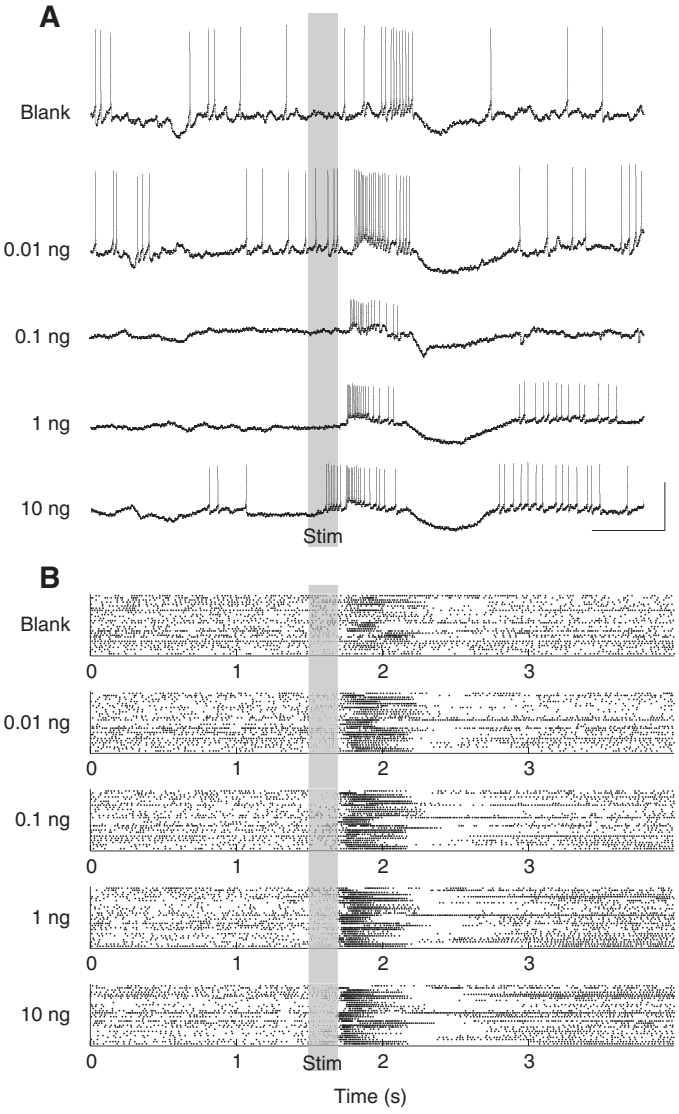

Fig. 7. Responses of macroglomerular complex (MGC) neurons to increasing stimulus loads of the main pheromone component (Z7-12:OAc). (A) Original recording. The grey bar indicates the stimulus duration (200 ms). Horizontal scale bar, 500 ms; vertical scale bar, 10 mV. (B) Raster plots for 29 MGC neurons. Each row represents the spikes emitted by a single neuron. The grey bar indicates the time during which the compound was applied (200 ms). The response pattern, an excitatory phase followed by an inhibitory phase, is conserved across the different doses.

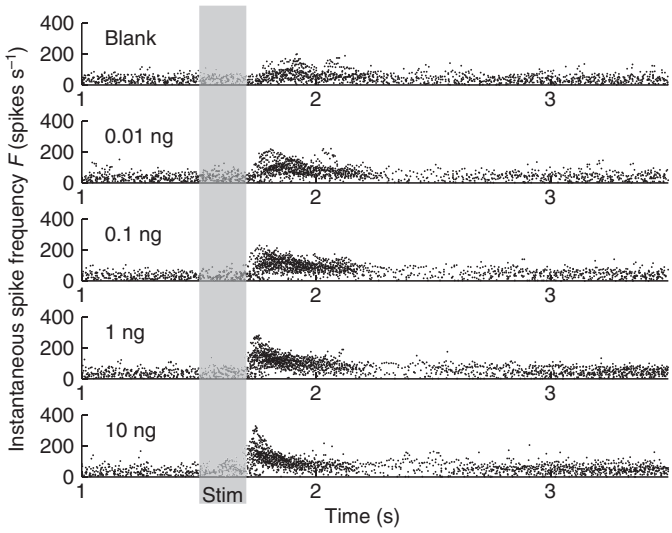

Fig. 8. Temporal response patterns of 29 macroglomerular complex (MGC) neurons to a 0.2 s stimulation with the solvent (blank) and doses of 0.01 ng, 0.1 ng, 1 ng and 10 ng of Z7-12:OAc. Each dot represents the instantaneous frequency F of a spike plotted against its time of occurrence. With increasing stimulus loads, neuron responses change from tonic to phasic–tonic. Latency L_1 decreases with increasing stimulus loads. No changes are observed in the inhibitory phase (visible as the period with the lowest density of dots). The grey bar indicates the time during which the compound was applied (200 ms).

The present results will serve to study the neural mechanisms underlying sensitivity changes as a function of the physiological state or experience.

Homogeneous PN response patterns

The results of this study show a uniform response pattern of the recorded neurons. As previously observed in *A. ipsilon* (Gadenne and Anton, 2000), the recorded neurons responded to the pheromone stimulation with an excitatory phase followed by an inhibitory phase. This pattern was found in 97% of the recorded neurons and was conserved even when the stimulus properties were changed (i.e. nature of components, stimulus load and duration of the stimulation) (Figs 6 and 7). In neurons responding to more than one pheromone component, all components yielded the typical response pattern previously described. The stained neurons presenting this response pattern always showed morphological characteristics of projection neurons. Moreover, neurons stained in other experiments presenting morphological characteristics of local neurons never showed the biphasic pattern described. These arguments indicate strongly that the neurons presented in this study are indeed PN. The type of morphology of these PN has been described as PIa(MGC) in *Helicoverpa zea* and *M. sexta* (Christensen et al., 1991; Homberg et al., 1988). The cell body of the PIa(MGC) neurons is located in the medial cluster and their axon projects *via* the inner antennocerebral tract to the mushroom bodies and the lateral protocerebrum. The inhibitory phase is a typical feature in the response of these PN. This has been observed in MGC neurons of many other insect species such as *A. segetum* (Hartlieb et al., 1997; Lei and Hansson, 1999; Wu et al., 1996), *M. sexta* (Matsumoto and Hildebrand, 1981) and *Drosophila melanogaster* (Wilson and Laurent, 2005). No quiescent period – i.e. a period in which no spike was generated – was clearly observed after excitatory responses of the ORNs in *A. ipsilon* (Renou et al., 1996) or in other moth species such as *Argyrotaenia velutinana* (O'Connell, 1975) and *S. littoralis* (Quero et al., 1996). This suggests that the inhibition phase observed in the PN resulted from synaptic interactions in the antennal lobe network. Moreover, no inhibitory postsynaptic potential preceding the excitatory phase, as in *M. sexta* (Christensen and Hildebrand, 1987; Waldrop et al., 1987), was observed in PN responses in *A. ipsilon*, even during stimulation with a pheromone blend.

Evidence of a mechanosensory input

Most of the neurons responding to the pheromone components responded with the same pattern but with a lower frequency to a stimulation with the solvent (hexane) only (see Figs 3 and 7) or with a clean filter paper. This suggests that these neurons receive mechanical input as in AL neurons in the cockroach *Periplaneta*

Table 2. Physiological characteristics of the 29 neurons stimulated with the main pheromone component (Z7-12:OAc)

	Values	Number of neurons
Estimated stimulus load at threshold C_0	0.005±0.002 ng	22
Estimated stimulus load at saturation C_{es}	≥9.8±3.8 ng	22
Observed stimulus load at saturation C_s	0.6±0.1 ng	17
Dynamic range C_s–C_0	2.6±0.3 log ng	10
Dynamic range C_{es}–C_0	≥3.5±0.3 log ng	22
Maximum firing frequency F_{max} (near saturation)	114±9 spikes s^{-1}	17
Maximum number of spikes in the excitation phase (near saturation)	33±2	29
Minimum latency	241±10 ms	20
Mean duration of excitation phase for a 200-ms stimulation	356±11 ms	29
Mean duration of inhibition phase for a 200-ms stimulation	655±30 ms	29

Values are means ± s.e.m.

americana and the noctuid moth *S. littoralis*, where interactions between mechanical and odorant stimuli have been observed (Han et al., 2005; Zeiner and Tichy, 1998). In *S. littoralis*, intracellular recordings and stainings showed the existence of mechanosensory afferents arborising within AL glomeruli (Han et al., 2005), which might be at the origin of rapid interactions between odorant and mechanosensory stimuli.

An essential role for the major pheromone component

As shown previously in the MGC neuron population of *A. ipsilon* (Gadenne and Anton, 2000), a large proportion of the MGC neurons studied here are tuned to Z7-12:OAc, the main pheromone component (80% responding and 50% highly specific), corroborating the essential role of this component in the sexual communication in this species. In the peripheral olfactory system, mainly ORN responding to Z7-12:OAc were found (Renou et al., 1996), which indicates that the input to the AL concerning the major pheromone component is very strong. In the related species *A. segetum*, specific AL neurons were mostly tuned to the major component of its pheromone (Wu et al., 1996). In the noctuid moths *H. virescens* and *H. zea*, most of the PN responded to the major component, and all of these neurons had dendritic arborizations in the largest MGC glomerulus, the cumulus (Christensen et al., 1991; Christensen et al., 1995). Our findings, with six stained neurons responding to the Z7-12:OAc, arborising in the cumulus, suggest that this glomerulus would receive input from ORN specifically tuned to the major component. Among the two secondary components, more MGC neurons responded to Z9-14:OAc (43%) than to Z11-16:Ac (29%). In the case of neurons responding to different components, all three components triggered the previously described typical response pattern. However, the latency of the response or the action potential frequency changed slightly, which

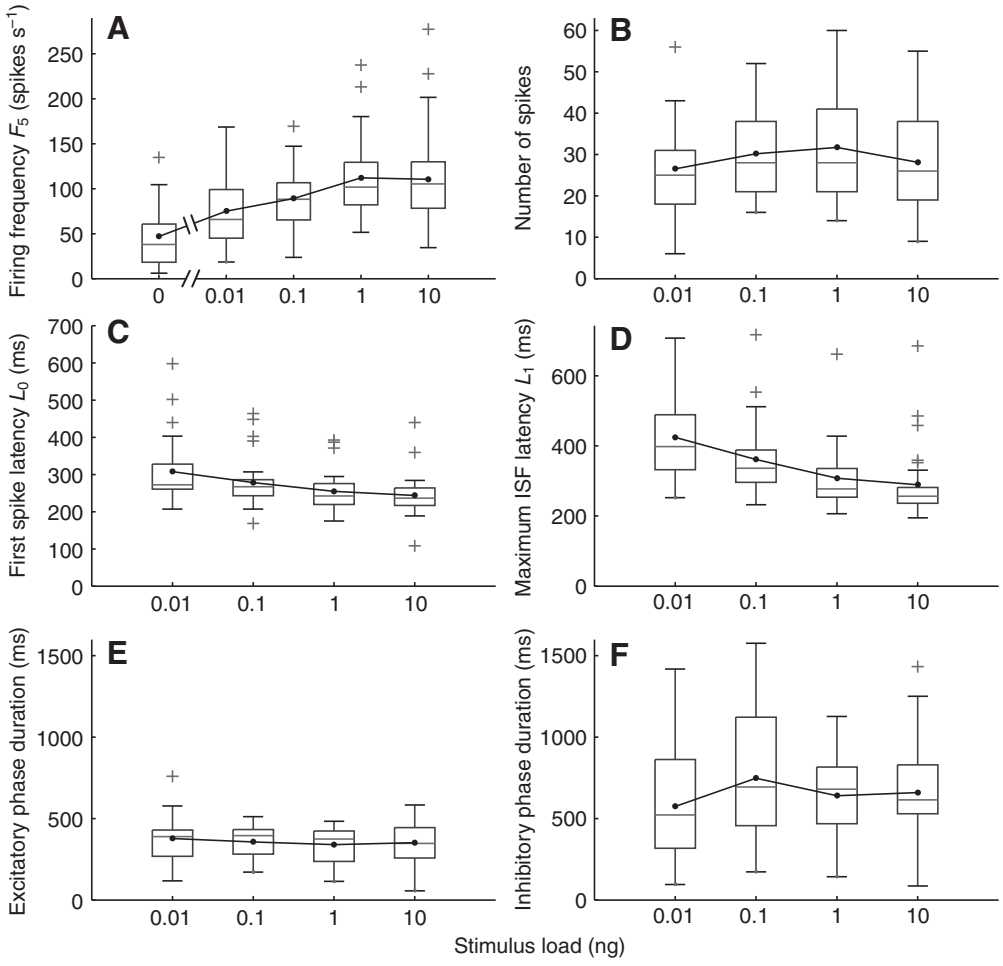

Fig. 9. Dose–response relationships represented by box plots for 29 macroglomerular complex (MGC) neurons stimulated with Z7-12:OAc. (A) Firing frequency (F_5). (B) Total number of spikes during the excitatory phase of the response. (C) Latency of the first spike of the response (L_0). (D) Latency (L_1) of the spike with highest instantaneous spike frequency (F_1). (E) Duration of the excitatory phase. (F) Duration of the inhibitory phase. On each plot, the box represents the interquartile range (IQR) of the data, the horizontal line inside the box represents the median, and the black dot represents the mean. The whiskers show the range of the remaining sample. Outliers (+) are observations greater than 1.5×IQR.

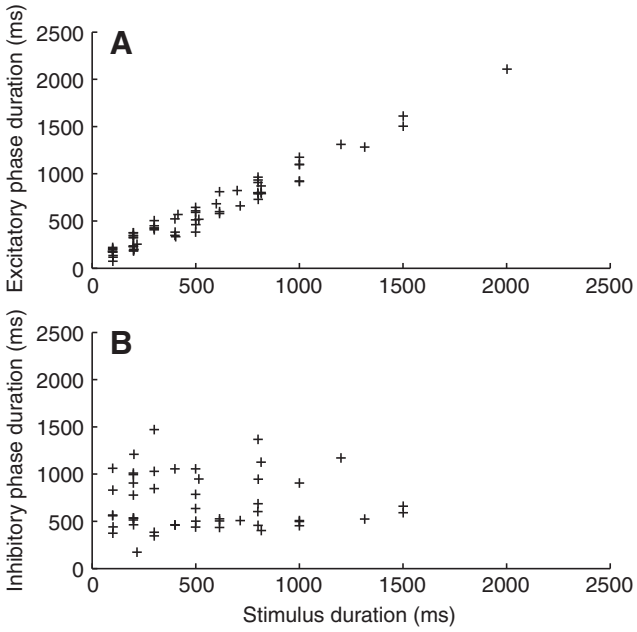

Fig. 10. Effect of the stimulus duration (0.01 ng, 0.1 ng and 1 ng of Z7-12:OAc) on the duration of (A) the excitatory phase (N=17 neurons) and (B) the inhibitory phase (N=15 neurons) of macroglomerular complex (MGC) neurons. Only the duration of the excitatory phase was found to be correlated with the stimulus duration.

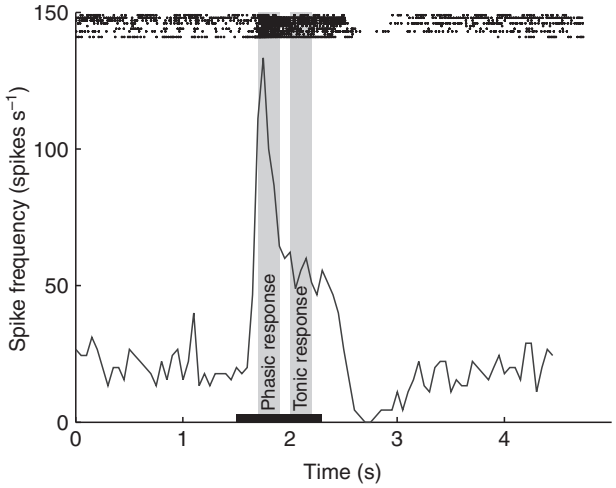

Fig. 11. Phasic–tonic pattern of macroglomerular complex (MGC) neuron responses. The figure shows the spike frequency (calculated from the number of spikes per 50-ms bin) averaged across responses of nine neurons to a 800-ms stimulation with the major component (same doses as in Fig. 10). Here, the division of the response into a phasic and a tonic part is clearly visible. Spike frequency was averaged in two bins of 200 ms (vertical grey bars), 200 ms and 500 ms after the stimulus onset. The frequency in the first bin was 107±5 spikes s^{-1} and in the second bin, 56±9 spikes s^{-1}. The horizontal black bar indicates the time during which the stimulus was applied.

suggests that some characteristics in the response of a single projection neuron could convey information about the nature of the components.

Although all three pheromone components are necessary to elicit behavioural attraction of males (Causse et al., 1988), an important role of Z7-12:OAc (major component, many ORN tuned to this component) has previously been described in the plasticity of central processing. Whereas the sensitivity of MGC neurons to the minor pheromone components (fewer ORN tuned to these components) is rather constant, the sensitivity of the MGC neurons responding to the major component changes as a function of the hormonal state (Gadenne and Anton, 2000).

Key parameters for odour intensity coding

Almost all quantitative properties of the excitatory phase in the PN response depend on the dose of the stimulus. The frequency, number of spikes and latency of the response convey information about the dose, whereas the durations of both the excitatory phase and the inhibitory phase do not seem to be affected by the dose.

The lowest tested dose leading to a response was 1 pg for the main component with a few neurons (data not shown) and the mean stimulus load at estimated threshold was ~5 pg. Some neurons might even have a lower threshold, as shown previously (Gadenne and Anton, 2000). When testing the main component on ORN, the stimulus load needed to elicit a response was ~1 ng for most of the neurons (D.J., P. Lucas, C.G., J.-P.R. and S.A., unpublished data). Similarly, in the related species *A. segetum*, the threshold of MGC neurons for the major component of the blend is at least 1000-fold lower than the threshold of the ORN (Wu et al., 1995; Wu et al., 1996). The very low amount of pheromone needed to elicit a response in MGC neurons can be interpreted as the consequence of the convergence of many ORN onto a lower number of PN in *A. ipsilon*. This convergence is a common property of the ORN:PN connections, as shown previously in other insect species (Hansson and Christensen, 1999; Hartlieb et al., 1997; Homberg et al., 1989; Rospars, 1988).

An increase of the stimulus dose led to an increase of the frequency and number of spikes in the excitatory phase. The dose–response relationship for most neurons was a sigmoid curve, as previously shown in studies of intensity coding (Christensen et al., 1991; Hartlieb et al., 1997; Kanzaki et al., 1989). These variables showed a plateau in the dose–response curves beginning at 1 ng of Z7-12:Oac, suggesting a saturation of the neurons at this dose. The increase in stimulus load induced a larger change in the frequency of the first spikes of the response (as reflected by the firing frequency F_5) than in the total number of spikes, suggesting that the information regarding the intensity might preferentially be processed in the first 100 ms.

The latency of the first spike of the response decreases with increasing doses, suggesting that a larger number of ORN fires spikes with a shorter latency to the stimulus at higher doses, which lets PN reach their depolarization threshold more rapidly. This suggests that the latency of the response could likely be used by protocerebral neurons to evaluate intensity.

The increase of stimulus intensity had no effect on either the duration of the excitatory phase or the whole response duration. These observations in PN are in clear contrast with ORN responses in other moth species; when the pheromone dose increased, most ORN responses increased both in intensity and duration (Berg et al., 1995; Kaissling, 1974). Therefore, the end of the excitatory phase of PN is likely not correlated with the end of the ORN response. This is in support of the idea that an inhibitory input from the AL network terminates the excitatory phase. Several lines of evidence suggest that LN are responsible for the inhibitory phase in the PN response pattern (Christensen et al., 1993; MacLeod and Laurent, 1996; Olsen and Wilson, 2008; Wilson and Laurent, 2005).

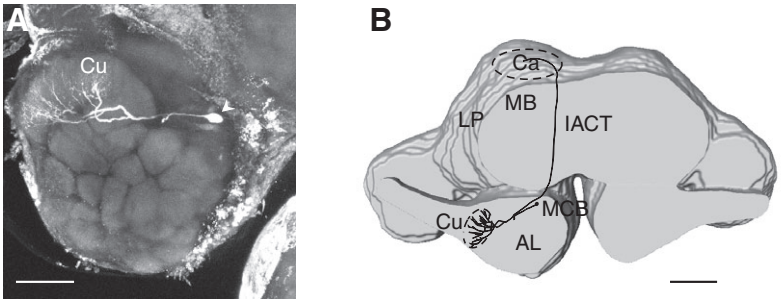

Fig. 12. Morphology of a pheromone-responding projection neuron (PN) stained with Neurobiotin™. (A) Maximum projection of 161 frontal optical sections through the antennal lobe, showing a stained PN arborising in the cumulus (Cu) of the macroglomerular complex (MGC). The cell body (arrowhead) is situated in the medial cell body cluster. Scale bar, 100 μm. (B) Three-dimensional reconstruction of the neuron in A in a frontal view, showing the axon projecting *via* the inner antennocerebral tract towards the calyces of the mushroom bodies. AL, antennal lobe; Ca, calyces of the mushroom bodies; Cu, cumulus; IACT, inner antennocerebral tract; LP, lateral protocerebrum; MB, mushroom bodies; MCB, medial cell body cluster. Scale bar, 200 μm.

Moreover, the stimulus duration is linearly related to the duration of the excitatory phase in *A. ipsilon* PN (Fig. 10A), in contrast to what was reported in *A. segetum* (Lei and Hansson, 1999), where the duration of the excitatory phase varied considerably with constant stimulation duration. The duration of inhibitory events in PN response patterns is not correlated with pheromone dose or stimulus duration.

Conclusions

Our characterization of the sex-pheromone responses of the PN of *A. ipsilon* males showed that the principal features of the pheromone signal are encoded by the characteristics of the excitatory phase. The analysed characteristics of the subsequent inhibitory phase did not show any relationship with the stimulus parameters. We therefore suggest that the inhibitory input provided by LN after the excitation phase might instead play a role in repolarizing PN rapidly and/or in synchronizing the PN responding to the same odour (Wilson and Laurent, 2005). These questions about the role of the different neuron types in the circuitry of the AL will be addressed in parallel studies on both LN and ORN. The precisely analysed dataset on virgin sexually mature males will be used to compare the responses of PN in males with other physiological states to elucidate the neural basis of the behavioural plasticity in the response to pheromones. In particular, we will compare the PN response patterns described here to those of sexually immature and of newly mated males that lack both behavioural and central nervous response sensitivity to the sex pheromone.

LIST OF SYMBOLS AND ABBREVIATIONS

AL	antennal lobe
C_0	stimulus load at threshold
Ca	calyces of the mushroom bodies
C_{es}	estimated stimulus load at saturation
C_s	stimulus load at saturation
Cu	cumulus of the macroglomerular complex
F	instantaneous spike frequency
F_1	maximum instantaneous spike frequency
F_S	firing frequency
F_{max}	maximum firing frequencies at high pheromone load
IACT	inner antennocerebral tract
ISI	interspike interval
L_0	latency of the first spike
L_1	latency of F_1
LN	local interneuron
LP	lateral protocerebrum
MB	mushroom bodies
MCB	medial cell body cluster
MGC	macroglomerular complex
ORN	olfactory receptor neuron
PN	projection neuron

We thank J. M. Nichols, L. Lloris, C. Chauvet and C. Gaertner for help with insect rearing and technical assistance. R. Barrozo, L. Couton, S. Minoli and N. Varela are acknowledged for their comments on an earlier version of the manuscript and help concerning the figures. This work was supported by research grants from INRA (Projet Jeune Equipe and Projet SPE) to S.A., C.G. and J.P.R. and from ANR-BBSRC 07 BSYS 006 (Pherosys) to J.P.R. and S.A., and by a Ph.D. grant from Université Pierre et Marie Curie to D.J.

REFERENCES

Anton, S. and Gadenne, C. (1999). Effect of juvenile hormone on the central nervous processing of sex pheromone in an insect. *Proc. Natl. Acad. Sci. USA* **96**, 5764-5767.

Anton, S. and Homberg, U. (1999). Antennal lobe structure. In *Insect Olfaction* (ed. B. S. Hansson), pp. 98-125. Berlin: Springer.

Anton, S., Löfstedt, C. and Hansson, B. S. (1997). Central nervous processing of sex pheromones in two strains of the European corn borer *Ostrinia nubilalis* (Lepidoptera: Pyralidae). *J. Exp. Biol.* **200**, 1073-1087.

Berg, B. G., Tumlinson, J. H. and Mustaparta, H. (1995). Chemical communication in heliothine moths. IV. Receptor neuron responses to pheromone compounds and formate analogues in the male tobacco budworm moth *Heliothis virescens*. *J. Comp. Physiol. A* **177**, 527-534.

Boeckh, J. and Selsam, P. (1984). Quantitative investigation of the odour specificity of central olfactory neurones in the American cockroach. *Chem. Senses* **9**, 369-380.

Causse, R., Buès, R., Barthes, J. and Toubon, J. (1988). Mise en évidence expérimentale de nouveaux constituants des phéromones sexuelles de *Scotia ipsilon* et *Mamestra suasa. Médiateurs chimiques: comportement et systématique des lépidoptères. Coll. INRA* **46**, 75-82.

Christensen, T. A. and Hildebrand, J. G. (1987). Male-specific, sex pheromone-selective projection neurons in the antennal lobes of the moth, *Manduca sexta*. *J. Comp. Physiol. A* **160**, 553-569.

Christensen, T. A., Mustaparta, H. and Hildebrand, J. G. (1991). Chemical communication in heliothine moths. II. Central processing of intra- and interspecific olfactory messages in the male corn earworm moth *Helicoverpa zea*. *J. Comp. Physiol. A* **169**, 259-274.

Christensen, T. A., Waldrop, B. R., Harrow, I. D. and Hildebrand, J. G. (1993). Local interneurons and information processing in the olfactory glomeruli of the moth *Manduca sexta*. *J. Comp. Physiol. A* **173**, 385-399.

Christensen, T. A., Mustaparta, H. and Hildebrand, J. G. (1995). Chemical communication in heliothine moths. VI. Parallel pathways for information processing in the macroglomerular complex of the male tobacco budworm moth *Heliothis virescens*. *J. Comp. Physiol. A* **177**, 545-557.

Gadenne, C. and Anton, S. (2000). Central processing of sex pheromone stimuli is differentially regulated by juvenile hormone in a male moth. *J. Insect Physiol.* **46**, 1195-1206.

Gadenne, C., Renou, M. and Sreng, L. (1993). Hormonal control of sex pheromone responsiveness in the male black cutworm, *Agrotis ipsilon*. *Experientia* **49**, 721-724.

Gadenne, C., Dufour, M. C. and Anton, S. (2001). Transient post-mating inhibition of behavioural and central nervous responses to sex pheromone in an insect. *Proc. Biol. Sci.* **268**, 1631-1635.

Gemeno, C. and Haynes, K. F. (1998). Chemical and behavioral evidence for a third pheromone component in a north american population of the black cutworm moth, *Agrotis ipsilon*. *J. Chem. Ecol.* **24**, 999-1011.

Gemeno, C., Anton, S., Zhu, J. W. and Haynes, K. F. (1998). Morphology of the reproductive system and antennal lobes of gynandromorphic and normal black cutworm moths, *Agrotis ipsilon* (Hufnagel) (Lepidoptera:Noctuidae). *Int. J. Insect Morphol. Embryol.* **27**, 185-191.

Greiner, B., Gadenne, C. and Anton, S. (2004). Three-dimensional antennal lobe atlas of the male moth, *Agrotis ipsilon*: a tool to study structure–function correlation. *J. Comp. Neurol.* **475**, 202-210.

Han, Q., Hansson, B. S. and Anton, S. (2005). Interactions of mechanical stimuli and sex pheromone information in antennal lobe neurons of a male moth, *Spodoptera littoralis*. *J. Comp. Physiol. A* **191**, 521-528.

Hansson, B. S. and Christensen, T. A. (1999). Functional characteristics of the antennal lobe. In *Insect olfaction* (ed. B. S. Hansson), pp. 125-161. Berlin: Springer-Verlag.

Hansson, B. S., Almaas, T. J. and Anton, S. (1995). Chemical communication in heliothine moths. V. Antennal lobe projection patterns of pheromone-detecting olfactory receptor neurons in the male *Heliothis virescens* (Lepidoptera: Noctuidae). *J. Comp. Physiol. A* **177**, 535-543.

Hartlieb, E., Anton, S. and Hansson, B. S. (1997). Dose-dependent response characteristics of antennal lobe neurons in the male moth *Agrotis segetum* (Lepidoptera: Noctuidae). *J. Comp. Physiol. A* **181**, 469-476.
Heinbockel, T., Christensen, T. A. and Hildebrand, J. G. (2004). Representation of binary pheromone blends by glomerulus-specific olfactory projection neurons. *J. Comp. Physiol. A* **190**, 1023-1037.
Homberg, U., Montague, R. A. and Hildebrand, J. G. (1988). Anatomy of antenno-cerebral pathways in the brain of the sphinx moth *Manduca sexta*. *Cell Tissue Res.* **254**, 255-281.
Homberg, U., Christensen, T. A. and Hildebrand, J. G. (1989). Structure and function of the deutocerebrum in insects. *Annu. Rev. Entomol.* **34**, 477-501.
Johansson, B. G. and Jones, T. M. (2007). The role of chemical communication in mate choice. *Biol. Rev.* **82**, 265-289.
Kaissling, K. E. (1974). Sensory transduction in insect olfactory receptors. In *Biochemistry of Sensory Functions* (ed. L. Jaenicke), pp. 243-273. Berlin: Springer Verlag.
Kanzaki, R., Arbas, E. A., Strausfeld, N. J. and Hildebrand, J. G. (1989). Physiology and morphology of projection neurons in the antennal lobe of the male moth *Manduca sexta*. *J. Comp. Physiol. A* **165**, 427-453.
Kay, L. M. and Stopfer, M. (2006). Information processing in the olfactory systems of insects and vertebrates. *Semin. Cell Dev. Biol.* **17**, 433-442.
Lei, H. and Hansson, B. S. (1999). Central processing of pulsed pheromone signals by antennal lobe neurons in the male moth *Agrotis segetum*. *J. Neurophysiol.* **81**, 1113-1122.
MacLeod, K. and Laurent, G. (1996). Distinct mechanisms for synchronization and temporal patterning of odor-encoding neural assemblies. *Science* **274**, 976-979.
Matsumoto, S. G. and Hildebrand, J. G. (1981). Olfactory mechanisms in the moth *Manduca sexta*: response characteristics and morphology of central neurons in the antennal lobes. *Proc. Biol. Sci.* **213**, 249-277.
Mustaparta, H. (1996). Central mechanisms of pheromone information processing. *Chem. Senses* **21**, 269-275.
O'Connell, R. J. (1975). Olfactory receptor responses to sex pheromone components in the redbanded leafroller moth. *J. Gen. Physiol.* **65**, 179-205.
Olsen, S. R. and Wilson, R. I. (2008). Lateral presynaptic inhibition mediates gain control in an olfactory circuit. *Nature* **452**, 956-960.
Picimbon, J. F., Gadenne, C., Bécard, J. M., Clément, J. L. and Sreng, L. (1997). Sex pheromone of the french black cutworm moth, *Agrotis ipsilon* (Lepidoptera:Noctuidae): identification and regulation of a multicomponent blend. *J. Chem. Ecol.* **23**, 211-230.
Poitout, S. and Buès, R. (1974). Elevage de plusieurs espèces de lépidoptères sur milieu artificiel simplifié. *Ann. Zool. Ecol. Anim.* **2**, 79-91.
Quero, C., Lucas, P., Renou, M. and Guerrero, A. (1996). Behavioral responses of *Spodoptera littoralis* males to sex pheromone components and virgin females in wind tunnel. *J. Chem. Ecol.* **22**, 1087-1102.
Renou, M., Gadenne, C. and Tauban, D. (1996). Electrophysiological investigations of pheromone-sensitive sensilla in the hybrids between two moth species. *J. Insect Physiol.* **42**, 267-277.
Rospars, J. P. (1988). Structure and development of the insect antennodeutocerebral system. *Int. J. Insect Morphol. Embryol.* **17**, 243-294.
Wakamura, S., Struble, D. L., Matsuura, H., Sato, M. and Kegasawa, K. (1986). Sex pheromone of the black cutworm, *Agrotis ipsilon*: attractant synergist and improved formulation. *Appl. Entomol. Zool.* **21**, 299-304.
Waldrop, B., Christensen, T. A. and Hildebrand, J. G. (1987). GABA-mediated synaptic inhibition of projection neurons in the antennal lobes of the sphinx moth, *Manduca sexta*. *J. Comp. Physiol. A* **161**, 23-32.
Wilson, R. I. and Laurent, G. (2005). Role of GABAergic inhibition in shaping odor-evoked spatiotemporal patterns in the Drosophila antennal lobe. *J. Neurosci.* **25**, 9069-9079.
Wu, W. Q., Hansson, B. S. and Löfstedt, C. (1995). Electrophysiological and behavioural evidence for a fourth sex pheromone component in the turnip moth, *Agrotis segetum*. *Physiol. Entomol.* **20**, 80-92.
Wu, W., Anton, S., Löfstedt, C. and Hansson, B. S. (1996). Discrimination among pheromone component blends by interneurons in male antennal lobes of two populations of the turnip moth, *Agrotis segetum*. *Proc. Natl. Acad. Sci. USA* **93**, 8022-8027.
Zeiner, R. and Tichy, H. (1998). Combined effects of olfactory and mechanical inputs in antennal lobe neurons of the cockroach. *J. Comp. Physiol. A* **182**, 467-473.